International Journal of Microwave and Wireless Technologies, 2017, 9(7), 1481–1487. © Cambridge University Press and the European Microwave Association, 2017
doi:10.1017/S1759078717000186

RESEARCH PAPER

Passive intermodulation model and experimental verification of cascaded microwave devices

TUANJIE LI[1], KAI ZHANG[1] AND JIE JIANG[2]

Passive intermodulation (PIM) is a complex problem in high-power microwave devices and satellite communications. In this paper, an effective calculation method is proposed for predicting PIM power levels of the cascaded microwave devices. First of all, the analytical formula of intermodulation voltage is derived based on the nonlinear I–V characteristics of microwave devices. Then, the mathematical model of point sources is constructed by the transmission line theory and extended to the cascaded microwave devices. The passive intermodulation products (PIMP) of the cascaded microwave devices are evaluated based on the point-source model. The relationship of PIM between a single microwave device and the cascaded system is revealed. Eventually, the corresponding experiments are designed to verify the accuracy of point-source model and the cascaded model to predict the third-order PIM power level, which address the problem of PIM prediction of the cascaded microwave devices.

Keywords: Microwave device, Passive intermodulation, Point-source model, Cascaded model

Received 22 May 2016; Revised 4 February 2017; Accepted 7 February 2017; first published online 8 March 2017

I. INTRODUCTION

In satellite communication systems, it is generally required that high-power multi-channel transmitters and super-sensitive broadband receivers be packed in a limited space. Because of the very large power level difference between transmit and receive signals and the limitation of frequency allocation, intermodulation (IM) interference due to passive residual nonlinearities in the high-power transmission path can be a real problem. The passive intermodulation products (PIMP) that fall into the receiving band will seriously degrade system performance [1, 2]. With the rapid development of communication technology and the extensive application of passive microwave devices, the passive intermodulation (PIM) gradually becomes more and more valued [3].

PIM distortion is caused by the inherent nonlinearity of microwave devices, which mainly involves contact nonlinearity and material nonlinearity [4]. Material nonlinearity mainly depends on the inherent nonlinear properties of materials with nonlinear conductive properties, such as ferromagnetic materials. Contact nonlinearity mainly depends on the contact form, temperature, vibration, and creep factors [5]. These factors are very complex, and all of them greatly influence PIM power levels.

[1]School of Mechano-Electronic Engineering, Xidian University, Xi'an 710071, China. Phone: +86 029 88202470
[2]Engineering College, Honghe University, Mengzi 661100, China
Corresponding author:
T. Li
Email: tjli888@126.com

Because of the complexity of PIM generation mechanism, many efforts focused on the effective analysis method for PIM. Brad and Rick [6] first put forward the concept of point-source model, by which the transmission characteristics of coaxial cables were equivalent to the transfer functions. Jargon *et al.* [7] proposed a PIM model for passive components in wireless base station based on *s*-parameters, which was a point-source model deduced from *s*-parameters. These models ignore many factors such as electric length, torque, and equipment noise, and cannot apply into the cascaded system.

In the microwave system, a large number of microwave devices are cascaded. There exist few researches about PIM of the cascaded system. Microwave connector is one of PIM sources. Although the linear properties of connectors have been well known [8], the contribution of their nonlinear characteristics to PIM is rarely introduced. Henrie *et al.* [9, 10] had carried out the more thorough research to PIM caused by the metal–metal contact in microwave connectors, and simply analyzed PIM of the cascaded connectors, and concluded several ways to reduce PIM. Kozlov *et al.* [11] built the equivalent circuit model based on the *x*-parameters and analyzed the nonlinearity of transmission lines, and the accuracy of the established model was verified by the adjacent channel power ratio and error vector magnitude. They [12] also tested the total nonlinearity of the cascaded distributed printed circuits, and studied the impacts of transmission line length and nonlinear capacitance on PIM. Zhao *et al.* [13] improved the point-source model by considering the effects of the length and loss of cables on PIM. The existing researches played a role in promoting PIM analysis of the

https://doi.org/10.1017/S1759078717000186 Published online by Cambridge University Press

cascaded system. This paper considers comprehensively the above-mentioned factors and puts forward a better PIM model of the cascaded microwave devices. The relationship of PIM between a single microwave device and the cascaded system is revealed for the convenience of engineering calculation.

An effective calculation method is proposed for predicting PIM power levels of the cascaded microwave devices in this work. In Section II, the analytical formula of IM voltage is derived. The point-source model is constructed and extended to the cascaded microwave devices. In Section III, the corresponding experiments are designed to verify the accuracy of the point-source model and the cascaded model. Section IV concludes and discusses the research work.

II. PIM MODEL OF CASCADED MICROWAVE DEVICES

A) IM voltage

Nonlinear devices do not obey Ohm's law, and the nonlinear current–voltage follows the power series [10, 14, 15].

$$I = f(V) = \sum_{n=1}^{m} a_n V^n, \tag{1}$$

where V is the voltage across the nonlinear device, I is the current through the nonlinear device, a_n ($n = 1, 2, \ldots, m$) are the coefficients of the power series, and a_3/a_1 represents the degree of third-order PIMP.

For the two carriers, we have

$$\begin{aligned} V &= V_1 \cos \omega_1 t + V_2 \cos \omega_2 t \\ &= \frac{1}{2} V_1 (e^{j\omega_1 t} + e^{-j\omega_1 t}) + \frac{1}{2} V_2 (e^{j\omega_2 t} + e^{-j\omega_2 t}) \\ &= \frac{1}{2} (V_1 e^{j\omega_1 t} + V_2 e^{j\omega_2 t}) + \frac{1}{2} (V_1 e^{-j\omega_2 t} + V_2 e^{-j\omega_2 t}) \\ &= \frac{1}{2} (E + E^*), \end{aligned} \tag{2}$$

where $E = V_1 e^{j\omega_1 t} + V_2\, e^{j\omega_2 t}$, E^* is the conjugate of E.

The binomial expansion of V^n is

$$V^n = \frac{1}{2^n} (E + E^*)^n = \frac{1}{2^n} \sum_{M_o=0}^{n} \frac{n!}{M_o!(n - M_o)!} E^{n-M_o} (E^*)^{M_o}, \tag{3}$$

where M_o is the binomial variable.

The odd-order PIMP is considered because they have interference to system [16]. According to the binomial symmetry, equation (3) can be rewritten as

$$V^n = \frac{1}{2^n} \left[2\mathrm{Re} \sum_{M_o=0}^{(n-1/2)} \frac{n!}{M_o!(n - M_o)!} E^{n-M_o} (E^*)^{M_o} \right]. \tag{4}$$

At the same way, the binomial expansions of E^{n-M_o} and $(E^*)^{M_o}$ are

$$\begin{aligned} E^{n-M_o} &= (V_1 e^{j\omega_1 t} + V_2 e^{j\omega_2 t})^{n-M_o} \\ &= \sum_{M_1=0}^{n-M_o} \frac{(n - M_o)!}{M_1!(n - M_o - M_1)!} V_1^{n-M_o-M_1} V_2^{M_1} \\ &\quad \times \exp[j((n - M_o - M_1)\omega_1 + M_1 \omega_2)t], \end{aligned} \tag{5}$$

$$\begin{aligned} (E^*)^{M_o} &= (V_1 e^{-j\omega_1 t} + V_2 e^{-j\omega_2 t})^{M_o} \\ &= \sum_{M_2=0}^{M_o} \frac{M_o!}{M_2!(M_o - M_2)!} V_1^{M_o-M_2} V_2^{M_2} \\ &\quad \times \exp[-j((M_o - M_2)\omega_1 + M_2 \omega_2)t], \end{aligned} \tag{6}$$

where M_1 and M_2 are the binomial variables.

Substituting equations (5) and (6) into (4), the expression of V^n including all frequency components is obtained as follows:

$$\begin{aligned} V^n = \frac{1}{2^n} \mathrm{Re} & \sum_{M_o=0}^{(n-1/2)} \frac{n!}{M_o!(n - M_o)!} \\ & \times \sum_{M_1=0}^{n-M_o} \frac{(n - M_o)!}{M_1!(n - M_o - M_1)!} V_1^{n-M_o-M_1} V_2^{M_1} \\ & \times \exp[j((n - M_o - M_1)\omega_1 + M_1 \omega_2)t] \\ & \times \sum_{M_2=0}^{M_o} \frac{M_o!}{M_2!(M_o - M_2)!} V_1^{M_o-M_2} V_2^{M_2} \\ & \times \exp[-j((M_o - M_2)\omega_1 + M_2 \omega_2)t]. \end{aligned} \tag{7}$$

The above formula can be simplified as

$$\begin{aligned} V^n = \frac{n!}{2^n} \sum_{M_o=0}^{(n-1/2)} \sum_{M_1=0}^{n-M_o} \sum_{M_2=0}^{M_o} & \frac{V_1^{n-M_1-M_2} V_2^{M_1+M_2}}{M_1! M_2! (n - M_o - M_1)! (M_o - M_2)!} \\ & \times \cos[(n - 2M_o - M_1 + M_2)\omega_1 + (M_1 - M_2)\omega_2]t. \end{aligned} \tag{8}$$

The frequency of PIMP is a linear combination of carrier frequencies, that is

$$\omega_{IM} = Q\omega_1 + R\omega_2, \tag{9}$$

where Q and R are the arbitrary integers.

From equations (8) and (9), there are

$$n - 2M_o - M_1 + M_2 = Q, \tag{10}$$

$$M_1 - M_2 = R. \tag{11}$$

From equations (10) and (11), we have

$$M_o = \frac{n - Q - R}{2}. \tag{12}$$

Substituting equations (11) and (12) into (8), we get

https://doi.org/10.1017/S1759078717000186 Published online by Cambridge University Press

$$V^n = \frac{n!}{2^n} \sum_{M_2=0}^{(n-Q-R/2)} \frac{V_1^{n-R-2M_2} V_2^{R+2M_2}}{(R+M_2)!M_2!(n-(n-Q-3R/2)-M_2)!((n-Q-R/2)-M_2)!} \cos[Q\omega_1 + R\omega_2]t. \quad (13)$$

According to the relationship between power and voltage,

$$P = 10\log_{10}\left(\frac{V^2}{2Z_o}\right) + 30, \quad (14)$$

we can derive the input voltage for the input power, where Z_o is the characteristic impedance.

From equation (1), we derive the analytic expression of the nth-order IM voltage as follows.

$$V_{IM} = \frac{a_n}{a_1} V^n. \quad (15)$$

Substituting equations (13) and (14) into (15), we can obtain the nth-order IM voltage.

B) PIM model of cascaded system

1) GENERAL MODEL

In the actual measurement, besides PIM source of microwave device under test (DUT), there are two kinds of unwanted PIM sources existing in the measurement result. One is the residual IM of measurement system, and the other is the self-interference of IM signal resulting from reflection [17]. Thus, the microwave network model of the cascaded system is established, as shown in Fig. 1, each DUT is regarded as a point resource.

The IM distortion results from the voltage waves caused by the nonlinearities of DUT. In Fig. 1, V_{IM}^k, V_{IM}^{k+}, and V_{IM}^{k-} represent the IM voltage, forward-propagating IM voltage and reverse-propagating (reflected) IM voltage of the kth ($k = 1, 2, \ldots, N$) DUT (point source), respectively. N is the number of DUTs. The electrical length l_{co} is the distance from the first nonlinear DUT to the instrument port. The electrical length l_{ck} is the distance between two DUTs. The electrical length l_l is the distance from the last nonlinear DUT to the low IM load, Z_L. Z_o is the characteristic impedance. Γ is the reflection coefficient. V_f and V_l represent the IM voltages of instrument and load, respectively.

Assuming all PIM sources have not secondary reflection, when $N = 1$, the forward-propagating IM voltage is

$$V_{IM}^{1+} = V_{IM}^1. \quad (16)$$

If the reflected PIM measurement method is adopted, then the phase difference of signal through cable should be considered. So the reflected IM voltage is [6]

$$V_{IM}^{1-} = V_{IM}^1 \exp(2j\beta l_{co}), \quad (17)$$

where β is the propagation constant.

With this in mind, the reflected IM voltage, V^-, at the receiver, as shown in Fig. 1, is expressed as

$$\begin{aligned} V^- = {} & V_f + V_{IM}^1 \exp[2j\beta l_{co}] + V_l \exp[2j\beta(l_{co} + l_l)] \\ & + \Gamma(V_f + V_{IM}^{1+} + V_l)\exp[2j\beta(l_{co} + l_l)]. \end{aligned} \quad (18)$$

When the several DUTs are cascaded [6], the IM voltage can be described as

$$V_{IMc}^+ = \sum_{k=1}^{N} V_{IM}^k, \quad (19)$$

$$V_{IMc}^- = \sum_{k=1}^{N} V_{IM}^k \exp\left[2j\beta\left(\sum_{s=1}^{k} l_{c(s-1)}\right)\right], \quad (20)$$

where V_{IMc}^+ is the total forward-propagating IM voltage, V_{IMc}^- is the total reverse-propagating IM voltage.

Equation (18) can be rewritten as

$$\begin{aligned} V^- = {} & V_f + \sum_{k=1}^{N}\left[V_{IM}^k \exp(2j\beta\left(\sum_{s=1}^{k} l_{c(s-1)}\right)\right] \\ & + V_l \exp\left[2j\beta\left(\sum_{k=1}^{N} l_{c(k-1)} + l_l\right)\right] \\ & + \Gamma\left(V_f + \sum_{k=1}^{N} V_{IM}^k + V_l\right)\exp\left[2j\beta\left(\sum_{k=1}^{N} l_{c(k-1)} + l_l\right)\right]. \end{aligned} \quad (21)$$

Because $a_n \ll a_1$ ($n > 1$) in the nonlinear I–V characteristics, the impedance of point source of the kth DUT can be

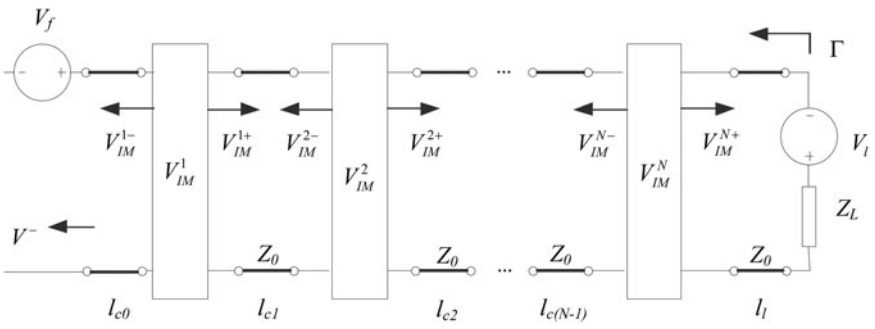


Fig. 1. Microwave network model of the cascaded system.

https://doi.org/10.1017/S1759078717000186 Published online by Cambridge University Press

simplified as

$$Z_{IM}^k = \frac{V^k}{I^k} = \frac{1}{a_1}, \tag{22}$$

where V^k and I^k are the voltage and current of the kth DUT, respectively.

According to the relation between power and voltage, we derive the PIM power level as follows:

$$P_{IM} = \frac{(V^-)^2}{2\sum_{k=1}^N Z_{IM}^k}. \tag{23}$$

Substituting equations (21) and (22) into (23), we can obtain the analytic expression of PIM power level of the cascaded system.

In order to further study PIM relationship between a single DUT and the cascaded system, equation (23) can be expanded as

$$\begin{aligned} P_{IM} =& \frac{1}{2\sum_{k=1}^N Z_{IM}^k}\left(V_f + \sum_{k=1}^N\left(V_{IM}^k \exp\left(2j\beta\left(\sum_{s=1}^k l_{c(s-1)}\right)\right)\right)\right. \\ &+ V_l \exp\left(2j\beta\left(\sum_{k=1}^N l_{c(k-1)} + l_l\right)\right) \\ &\left.+ \Gamma\left(V_f + \sum_{k=1}^N V_{IM}^k + V_l\right)\exp\left(2j\beta\left(\sum_{k=1}^N l_{c(k-1)} + l_l\right)\right)\right)^2 \\ =& \frac{1}{2\sum_{k=1}^N Z_{IM}^k}\left(C_f^2 (V_f)^2 + \sum_{k=1}^N C_k^2 (V_{IM}^k)^2 + C_l^2 (V_l)^2 + \Delta V^2\right), \end{aligned} \tag{24}$$

where, C_f and C_l are the parameters of instrument and load, respectively, dependent on the phase of IM voltage. C_k is the parameters of the kth DUT dependent on the phase of IM voltage. ΔV^2 is the voltage remainder. They are expressed as

$$C_f = 1 + \Gamma \exp\left(2j\beta\left(\sum_{k=1}^N l_{c(k-1)} + l_l\right)\right), \tag{25}$$

$$C_k = \exp\left(2j\beta\left(\sum_{s=1}^k l_{c(s-1)}\right)\right) + \Gamma \exp\left(2j\beta\left(\sum_{k=1}^N l_{c(k-1)} + l_l\right)\right), \tag{26}$$

$$C_l = (1+\Gamma)\exp\left(2j\beta\left(\sum_{k=1}^N l_{c(k-1)} + l_l\right)\right), \tag{27}$$

$$\begin{aligned} \Delta V^2 =& 2C_f C_l V_f V_l + \sum_{i=1}^N 2C_f C_i V_f V_{IM}^i \\ &+ \sum_{j=1}^N 2C_l C_j V_l V_{IM}^j + \sum_{i=1}^{N-1}\sum_{j=i+1}^N (2C_i C_j V_{IM}^i V_{IM}^j). \end{aligned} \tag{28}$$

Substituting equation (23) into (24), the calculation formula of the PIM power level can be obtained as follows:

$$\begin{aligned} P_{IM} =& \frac{C_f^2 (V_f)^2}{2\sum_{k=1}^N Z_{IM}^k} + \frac{C_l^2 (V_l)^2}{2\sum_{k=1}^N Z_{IM}^k} \\ &+ \frac{\sum_{k=1}^N C_k^2 (V_{IM}^k)^2}{2\sum_{k=1}^N Z_{IM}^k} + \frac{\Delta V^2}{2\sum_{k=1}^N Z_{IM}^k} \\ =& C_f^2 P_f + C_l^2 P_l + \sum_{k=1}^N\left(C_k^2 P_k \cdot \frac{Z_{IM}^k}{\sum_{s=1}^N Z_{IM}^s}\right) + \Delta P, \end{aligned} \tag{29}$$

where P_f is the PIM power level of the instrument, P_l is the PIM power level of the load, P_k is the PIM power level of the kth DUT, and ΔP is the power remainder whose expression is

$$\begin{aligned} \Delta P =& \frac{1}{2\sum_{k=1}^N Z_{IM}^k}\left(2C_f C_l V_f V_l + \sum_{i=1}^N 2C_f C_i V_f V_{IM}^i \right. \\ &\left. + \sum_{j=1}^N 2C_l C_j V_l V_{IM}^j + \sum_{i=1}^{N-1}\sum_{j=i+1}^N (2C_i C_j V_i V_j)\right) \\ =& 2C_f C_l \sqrt{P_f P_l} + \sum_{i=1}^N\left(2C_f C_i \sqrt{\frac{Z_{IM}^i}{2\sum_{k=1}^N Z_{IM}^k}}\sqrt{P_f P_i}\right) \\ &+ \sum_{j=1}^N\left(2C_l C_j \sqrt{\frac{Z_{IM}^j}{2\sum_{k=1}^N Z_{IM}^k}}\sqrt{P_l P_j}\right) \\ &+ \sum_{i=1}^{N-1}\sum_{j=i+1}^N\left(2C_i C_j \frac{\sqrt{Z_{IM}^i Z_{IM}^j}}{2\sum_{k=1}^N Z_{IM}^k}\sqrt{P_i P_j}\right), \end{aligned} \tag{30}$$

where C_i and C_j are the parameters of the ith and jth DUTs, respectively, dependent on the phase of IM voltage, P_i and P_j are the PIM power levels of the ith and jth DUTs, respectively.

Equation (29) reveals the relationship of PIM power levels between a single DUT and the cascaded system. It can be seen that the PIM power level of the cascaded system nonlinearly increases with the number of cascaded DUTs.

2) SIMPLIFIED MODEL

When the nonlinear characteristics of all DUTs are nearly same, they would produce the identical PIMP under identical conditions such as same torques and working environment. Then, equations (19) and (20) can be simplified as

$$V_{IMc}^+ = NV_{IM}, \tag{31}$$

$$V_{IMc}^- = \sum_{k=1}^N [V_{IM} \exp(2j\beta((k-1)l_c + l_{co}))]. \tag{32}$$

https://doi.org/10.1017/S1759078717000186 Published online by Cambridge University Press

Equation (21) can be rewritten as

$$V^- = V_f + \sum_{k=1}^{N} [V_{IM} \exp(2j\beta((k-1)l_c + l_{co}))] + V_l \exp[2j\beta((N-1)l_c + l_{co} + l_l)] + \Gamma(V_f + NV_{IM} + V_l) \exp[2j\beta((N-1)l_c + l_{co} + l_l)], \quad (33)$$

where l_c is the electrical length between two DUTs.

Equation (23) can be simplified as

$$P_{IM} = \frac{(V^-)^2}{2NZ_{IM}}. \quad (34)$$

According to equations (33) and (34), PIM power levels of the cascaded system can be calculated.

Compared with the existing models, the proposed model could be applied into many situations, including the point sources and cascaded system, and considering the reflection, forward-propagation, electric length, equipment noise, etc.

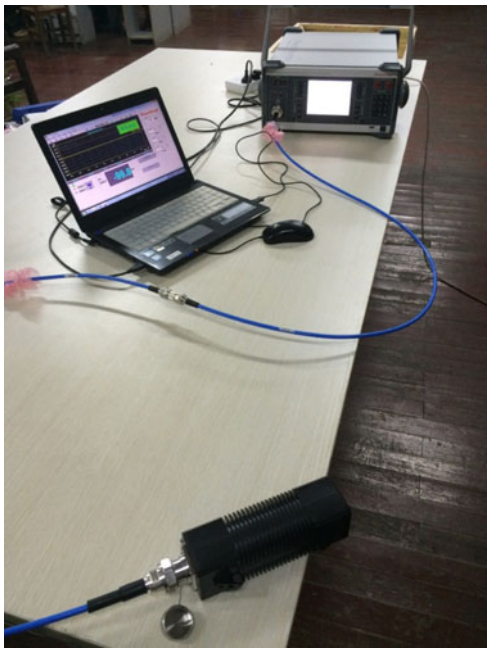


Fig. 2. Test connection diagram.

III. EXPERIMENT VALIDATION

A) Experimental equipment and principle

The input signal frequencies for measurement are $f_1 = 2620$ MHz and $f_2 = 2690$ MHz. The third-order PIMP with frequency $2f_1 - f_2 = 2550$ MHz will be measured at room temperature.

The experimental equipment includes the Rosenberger portable PIM tester, Rosenberger low PIM load, several Pasternack *N*-type coaxial connectors as DUTs, and low PIM test cable with characteristic impedance of 50 Ω. The torque acting on DUTs is 10 Nm, and the measurement error of torque is 0.5 Nm.

As shown in Fig. 2, the Rosenberger portable PIM tester is connected to DUT and low PIM load, the other port is connected to PC to show the results. The structure of test system is shown in Fig. 3.

B) Verification steps

For verifying the correctness of the proposed model, we design the following experimental verification steps:

(1) When $P_1 = P_2$, the third-order PIM power levels of a connector with different input powers are measured.
(2) When $P_1 \neq P_2$, the third-order PIM power levels of a connector with different ratios of two input powers are measured.
(3) The third-order PIM power levels with different number of cascaded DUTs are measured.
(4) The third-order PIM power level of a single DUT is measured when $P_1 = P_2 = 43$ dBm, then a_0 and a_3 can be determined. Substituting a_0 and a_3 into equations (15) and (22), the IM voltage and impedance of point source can be acquired. Let $C = n = 3$, $Q = 2$, $R = -1$, $l_{co} = l_l = 1.5$ m in equations (13), (14), and (33), and substituting V_1 and V_2 into equation (15), V_{IM3} can be obtained. Finally, by equation (23) the theoretical results of third-order PIM power levels of single DUT and cascaded DUTs can be obtained.

C) Results and discussion

The experimental and theoretical results in different conditions are shown in Figs 4 and 5.

As shown in Fig. 4(a), when $P_1 = P_2$ and for the different input powers, the calculated result of point-source model matches well with that of the experimental result. As shown in Fig. 4(b), when $P_1 \neq P_2$ and for the different ratios of two input powers, the slopes of third-order PIM power levels are −1 dB and 2 dB, respectively, which can be proven as follows.

For the third-order PIM, from equations (13) and (15), there are

$$V_{IM} \propto V_1^2 V_2. \quad (35)$$

From equations (23) and (35), the relationship between the third-order PIM power level and input powers can be obtained as

$$P_{IM} \propto P_1^2 P_2. \quad (36)$$

Further

$$P_{IM}(\text{dBm}) \propto 30 \log_{10}(P_1) - 10 \log_{10}(P_1/P_2), \quad (37)$$

$$P_{IM}(\text{dBm}) \propto 10 \log_{10}(P_2) + 20 \log_{10}(P_1/P_2). \quad (38)$$

It can be seen from equation (37) that the slope of the third-order PIM power level is −1 dB, when P_1 is constant. From equation (38) the slope of the third-order PIM power level is 2 dB, when P_2 is constant.

https://doi.org/10.1017/S1759078717000186 Published online by Cambridge University Press

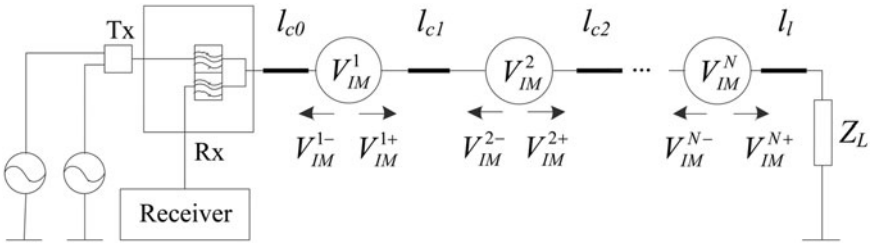


Fig. 3. Structure of the test system.

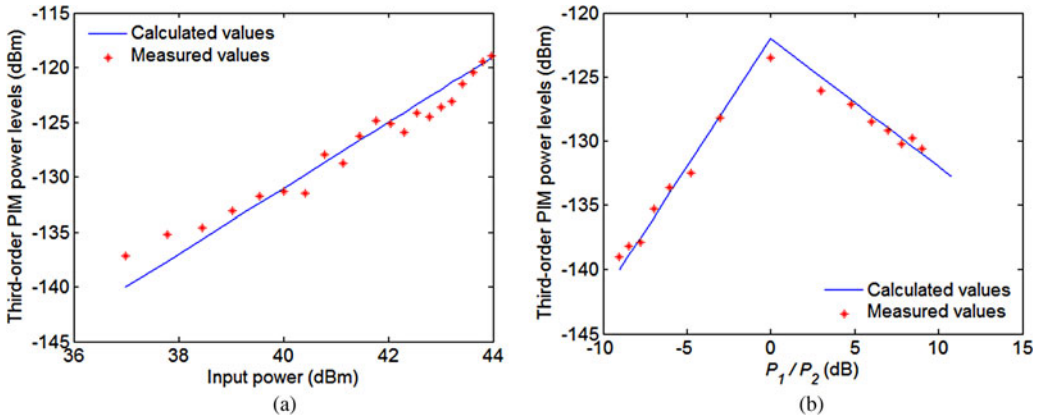


Fig. 4. Comparison of the experimental and calculated values of third-order PIM power levels. (a) The third-order PIM power levels when $P_1 = P_2$. (b) The third-order PIM power levels with different ratios of two input powers.

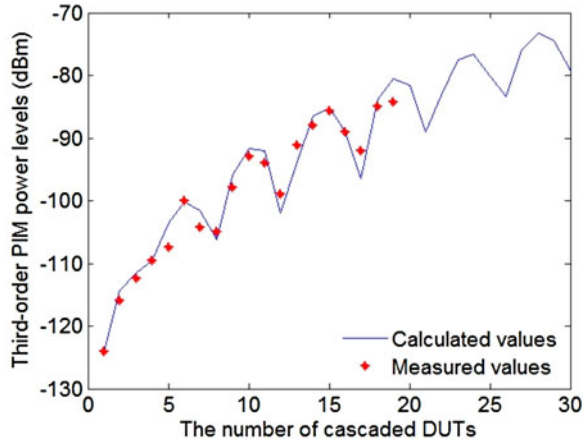


Fig. 5. Comparison of experimental and calculated values of third-order PIM power levels of cascaded DUTs.

The above results indicate the point-source model can accurately predict PIM power levels with different input powers.

As shown in Fig. 5, the third-order PIM power levels of different number of cascaded DUTs are measured. Although, there are some discrepancies between the experimental and calculated values because of the measurement errors among the torques acting on the cascaded DUTs, on the whole, the experimental results are consistent with the theoretical values, which indicate the cascaded model can accurately predict PIM power levels of the cascaded system. There exist some oscillations because the cascaded model considers the phase change of IM voltage.

IV. CONCLUSIONS

(1) This paper introduces a solving method of IM voltage based on the nonlinear I–V characteristics of microwave devices. The point-source model is constructed by the transmission line theory. The consistence between the theoretical values and experimental results validates the point-source model.
(2) The point-source model is extended to the cascaded microwave devices and PIM power levels are predicted. The relationship of PIM power levels between a single microwave device and the cascaded system is revealed. The comparison of experimental and calculated values verifies the correctness of the cascaded model.
(3) The developed models comprehensively consider the error sources such as the IM residual of system, IM reflection and IM voltage phase, etc. The developed models are universal and provide an effective calculation method for predicting PIM power levels of the large-scale cascaded system.

REFERENCES

[1] Shitvov, A.; Schuchinsky, A.G.; Steer, M.B.; Wetherington, J.M.: Characterisation of nonlinear distortion and intermodulation in passive devices and antennas, in Eur. Conf. on Antennas and Propagation, 2014, 1454–1458.

[2] Bolli, P.; Selleri, S.; Pelosi, G.: Passive intermodulation on large reflector antennas. IEEE Antennas Propag. Mag., **44** (2002), 13–20.

[3] Lui, P.L.: Passive intermodulation interference in communication systems. Electron. Commun. Eng. J., **2** (1990), 109–118.

https://doi.org/10.1017/S1759078717000186 Published online by Cambridge University Press

[4] Rezvanian, O.; Zikry, M.A.; Brown, C.; Krim, J.: Surface roughness, asperity contact and gold RF MEMS switch behavior. J. Micromech. Microeng., **17** (2007), 2006–2015.

[5] Bond, C.D.; Guenzer, C.S.; Carosella, C.A.: Intermodulation generation by electron tunneling through aluminum-oxide films. Proc. IEEE, **67** (1979), 1643–1652.

[6] Brad, D.; Rick, H.: Measuring the passive-IM performance of RF cable assemblies. Microw. RF, **36** (1997), 108–114.

[7] Jargon, J.A.; Degroot, D.C.; Reed, K.L.: NIST passive intermodulation measurement comparison for wireless base station equipment, in 52nd ARFTG Conf. Digest: Computer-Aided Design and Test for High-Speed Electronics, 1998, 128–139.

[8] Timsit, R.S.: High speed electronic connectors: a review of electrical contact properties. IEEE J. Quantum Electron., **E88-C** (2005), 1791–1798.

[9] Henrie, J.J.; Christianson, A.J.; Chappell, W.J.: Linear–nonlinear interaction and passive intermodulation distortion. IEEE Trans. Microw. Theory Tech., **58** (2010), 1230–1237.

[10] Henrie, J.J.; Christianson, A.J.; Chappell, W.J.: Prediction of passive intermodulation from coaxial connectors in microwave networks. IEEE Trans. Microw. Theory Tech., **56** (2008), 209–216.

[11] Kozlov, D.S.; Shitvov, A.P.; Schuchinsky, A.G.: On passive intermodulation test of analog and digital systems, in Integrated Nonlinear Microwave and Millimetre-wave Circuits Workshop, 2015, 1–3.

[12] Kozlov, D.S.; Shitvov, A.P.; Schuchinsky, A.G.: Passive intermodulation in distributed circuits with cascaded discrete nonlinearities, in Eur. Conf. on Antennas and Propagation, 2015, 1–5.

[13] Zhao, P.; Zhang, X.; Yang, D.; Hu, X.: Superposition effect of passive intermodulation for cable assemblies with discrete point-sources. China Commun., **12** (2015), 97–105.

[14] Jiang, J.; Li, T.; Liu, Y.: Passive inter-modulation scattering analysis of reflector considering contact nonlinearity. Chin. J. Aeronaut., **26** (2013), 463–469.

[15] Sui, W.; Christensen, D.A.; Durney, C.H.: Extending the two-dimensional FDTD method to hybrid electromagnetic systems with active and passive lumped elements. IEEE Trans. Microw. Theory Tech., **40** (1992), 724–730.

[16] Eng, K.Y.; Stern, T.E.: The order-and-type prediction problem arising from passive intermodulation interference in communications satellites. IEEE Trans. Commun., **29** (1981), 549–555.

[17] Hienonen, S.; Raisanen, A.V.: Effect of load impedance on passive intermodulation measurements. Electron. Lett., **40** (2004), 245–247.



Tuanjie Li received his Ph.D. degree from Xi'an University of Technology in 1999. He now is a Professor and Ph.D. supervisor at School of Mechano-Electronic Engineering, Xidian University. His main research interests are space deployable structures and passive intermodulation.



Kai Zhang received his Diploma in 2015 from Xi'an Shiyou University. He now is a master of instrument and meter engineering in Xidian University. His current research interests include microwave technique and passive intermodulation.



Jie Jiang received her Ph.D. degree from Xidian University in 2016. Now she is a teacher at Honghe University. Her current research interests include microwave technique and passive intermodulation.

https://doi.org/10.1017/S1759078717000186 Published online by Cambridge University Press